Sādhanā Vol. 33, Part 5, October 2008, pp. 671–687. © Printed in India

Design and analysis of full pitch winding and concentrated stator pole winding three-phase flux reversal machine for low speed application

D S MORE, HARI KALLURU and B G FERNANDES

Department of Electrical Engineering, Indian Institute of Technology Bombay, Powai, Mumbai 400 076
e-mail: dsmore@ee.iitb.ac.in; khari@ee.iitb.ac.in; bgf@ee.iitb.ac.in

Abstract. The flux reversal machine (FRM) is a doubly-salient stator permanent magnet machine with flux linkage reversal in the stator concentrated winding. The existing machines at low speed, low power (2·4 kW, 300 rpm) range are not economical. FRM topology is best suited for this application. An attempt has been made to improve the power density of machine by introducing full pitch winding. Full pitch winding FRM (FPFRM) has higher power density than the conventional concentrated stator pole winding FRM (CSPFRM).

Design and comparative analysis of FPFRM and CSPFRM are made. Both machines are designed for 88·58 Nm and 300 rpm. Design details of both machines are presented. Finite Element Method (FEM) analysis is carried out to evaluate and compare the performance of CSPFRM and FPFRM. Series capacitive compensation is provided for better voltage regulation of both machines.

Keywords. Flux reversal machine (FRM); full pitch winding; doubly salient permanent magnet electrical machine; finite-element method (FEM) analysis.

1. Introduction

Single-phase FRM was first introduced by Deodhar *et al* (1997) for an automobile application to replace the standard claw pole alternator. It has numerous advantages such as simple construction, low inertia and high power density. Three-phase FRM was introduced by Wang *et al* (1999). The design of the machine has been optimized to ensure (i) high PM flux linkage in the winding, (ii) low cogging torque and permanent magnet (PM) weight. The basic machine configuration is an 8 salient pole rotor and 6 salient pole stator with concentrated windings. Permanent Magnets are fixed to the stator pole. Figure 1 shows this machine configuration.

FRM for low-speed servo drive application was introduced by Boldea *et al* (2002). This low speed machine has 28 poles on the rotor and 12 on stator with two permanent magnet pairs on each stator pole. This machine is designed for 128 rpm at 60 Hz. Using vector control high torque density with less than 3% torque pulsation is achieved. In order to reduce the cogging torque, rotor teeth pairing method has been proposed (Kim *et al* 2005). Attempts were made to reduce the leakage flux by providing flux barrier on the rotor poles at its edges

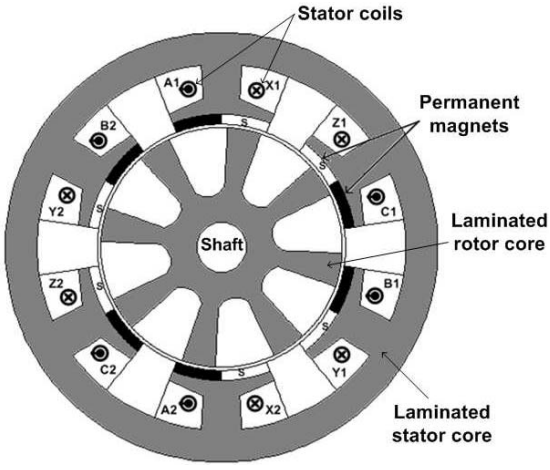

Figure 1. Cross-section of conventional 6/8 pole CSPFRM.

(Kim & Lee 2004). Power density comparison of doubly salient permanent magnet machines has been made. It is concluded that FRM has higher power density in comparison with other machines in the same class (Zhang *et al* 2006).

The need for increased use of renewable energy is well established. Small-scale wind turbines (rooftop) have the potential to provide electricity to domestic and commercial applications. Rooftop wind energy generation has acquired importance due to environmental concerns. These generators should be direct driven. Since cogging torque can be reduced by proper skewing of the rotor, acoustic noise can be reduced. This is one of the requirement for rooftop wind generation system.

Depending upon the output power, the variation in the rated speed of the rooftop wind turbine is 140 rpm to 500 rpm. Low capacity wind turbine has higher speed and as the capacity increases, the speed decreases. Rooftop wind power generation system has power rating variation from 0·6 kW to 15 kW. The rated speed of 2·4 kW machine is 300 rpm. So, prototype of the machine 2·4 kW, 300 rpm is designed.

In this paper, comparative analysis of low speed FPFRM and CSPFRM for the same power rating is made. FEM analysis using Flux 2D is carried out for both machines. Section 2 describes the basic operation of FRM. Full Pitch Winding FRM is discussed in § 3. Section 4 describes the design details of CSPFRM and FPFRM for low speed application and the 2D FEM analysis for calculating the self and mutual inductance is discussed in § 5. Section 6 describes the FEM analysis on load to determine the voltage regulation of both machines and a method used to improve the voltage regulation. Section 7 compares steady state motor performance of both machines and finally conclusions are drawn.

2. Flux reversal machine

The FRM is a doubly salient machine with permanent magnets on the stator. The PMs are fixed on the stator pole have opposite polarities and therefore as the rotor rotates PM flux linkage of the stator phase concentrated coils reverses the polarity under the same stator pole. Although the field excitation is provided by the permanent magnets, the flux linkage of the armature winding is modulated by the variation of the magnetic circuit reluctance as the rotor rotates in such a way that a bipolar EMF is induced without rotating magnets. Its simple

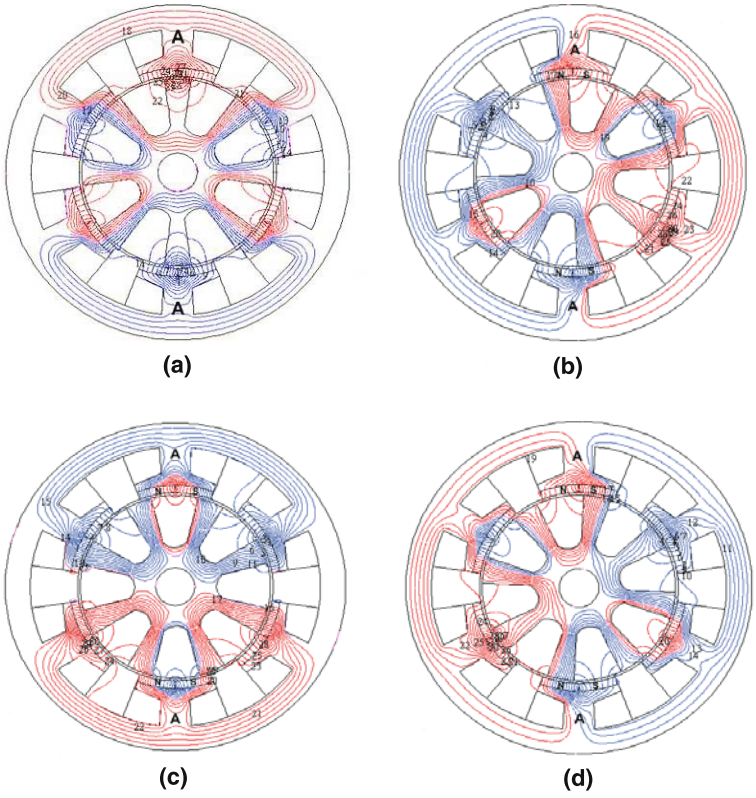

Figure 2. Operating principle of 6/8 pole FRM.

structure makes it cost effective and suitable for mass production. It has the advantages of switched reluctance machine (SRM) and permanent magnet synchronous machine (PMSM) (Deodhar *et al* 1997).

The principle of operation of 6/8 pole FRM is explained as follows: Figure 2a is an equilibrium position for A-phase, where the flux set-up by the magnets circulates entirely within A-phase stator pole, and there is no flux in the A-phase stator teeth. In this position no flux links with the A-phase coil. In figure 2b, the rotor is displaced by 11·25° counter clockwise, so that the rotor pole aligns with one of the magnets. The flux now passes through the coils and the stator yoke. The flux linkage in A-phase is maximum at this position. In figure 2c, the rotor is at a second equilibrium position, displaced from the first one by 22·5°, where, again, there is no flux in the A-phase stator teeth and no flux linking the A-phase coils. In figure 2d, rotor further displaced by 11·25° in counter clockwise direction, where the phase flux is maximum in the direction opposite to the one shown in figure 2b. As the flux linking the stator winding is sinusoidal, the induced emf is also sinusoidal as shown in figure 3.

The frequency and speed relationship for FRM (Wang *et al* 1999) is given by

$$f = \frac{N \times P_r}{60}, \tag{1}$$

where N = rotor speed (rpm).

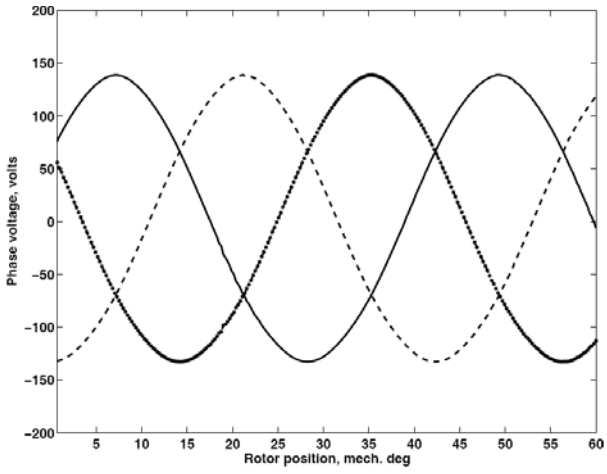

Figure 3. Induced EMF in 6/8 pole FRM.

P_r = number of rotor teeth or poles.
f = frequency of induced EMF (Hz).
Where as number of equivalent flux pattern poles (P_{eq}) is given by

$$P_{eq} = P_s/3, \tag{2}$$

where P_s = number of stator poles.

FRM machine with 6/8 pole has two effective poles, and hence in one cycle, flux pattern completes one revolution. Thus when rotor speed is N rpm, the flux pattern completes $P_r \times N$ revolutions per minute. Hence, flux pattern rotates P_r times the shaft speed. In conventional synchronous machine, flux pattern speed and rotor speed is same. Pictorial representation of FRM generator and permanent magnet synchronous generator is shown in figure 4. Both machine representation is for same speed and output frequency. Flux pattern in FRM rotating P_r times rotor speed can be represented as a fictitious step-up gear and is called as 'Electrical Gear'. Electrical gear ratio (K) is defined as the ratio of flux pattern speed to the shaft speed. The value of K is given as

$$K = \frac{P_r}{P_{eq}/2}. \tag{3}$$

Conventional synchronous machine should have $2 \times P_r$ poles for the same output frequency and rotor speed.

3. Full pitch winding flux reversal machine

Concept of fictitious 'Electrical Gear' in analysing the flux pattern in FRM and concept of full pitch winding for this machine was introduced. It was proved that full pitch winding increases the power density of the machine. Concept of fictitious electrical gear makes it possible to compare FRM with PMSM (More & Fernandes 2007).

The normal component of flux density at the middle of stator pole along the periphery of 6/14 pole FRM is shown in figure 5. The cross-section of 12/16 pole CSPFRM is given in figure 6. Machine configurations of 6/14 pole CSPFRM and FPFRM are shown in figures 7

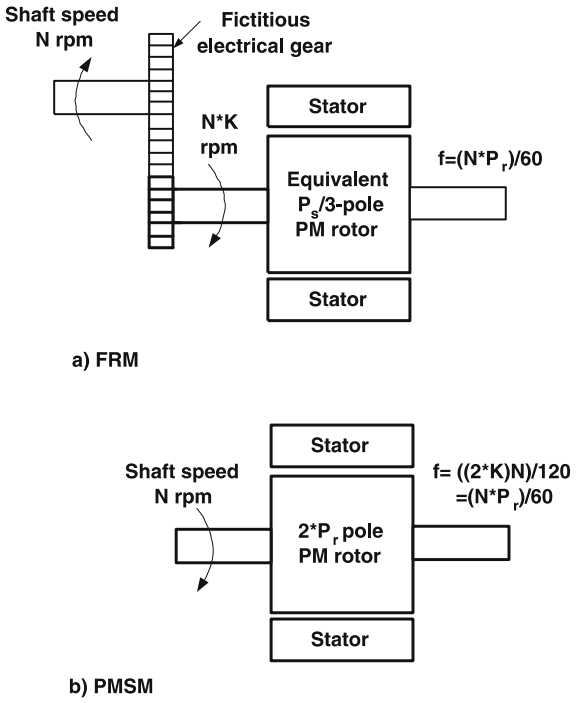

Figure 4. Representation of fictitious electrical gear in FRM.

and 8 respectively. The close look on the normal component of flux density plot reveals that the machine has two pole flux pattern. In other words, the machine has two effective poles. FRM has 6 slots, hence electrical angle per slot is 60°. Concentrated stator pole winding has a coil span of 60° elec. and therefore fundamental pitch factor of the (CSPFRM) stator winding is 0·5. As electrical angle between the slots is 60°, full pitch winding is possible. The arrangement of full pitch winding is shown in figure 8.

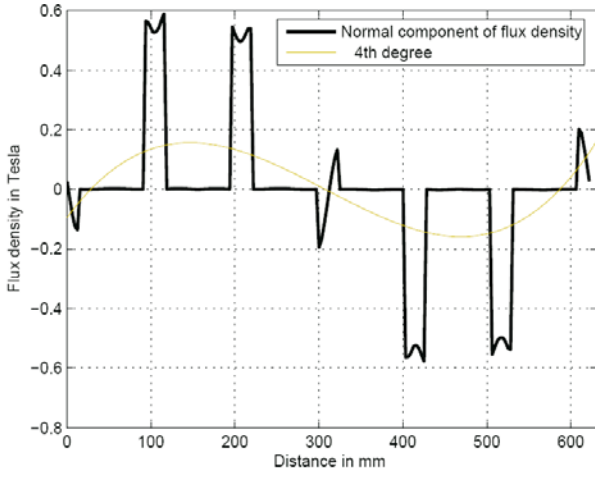

Figure 5. Normal component of flux density in 6/14 pole FRM.

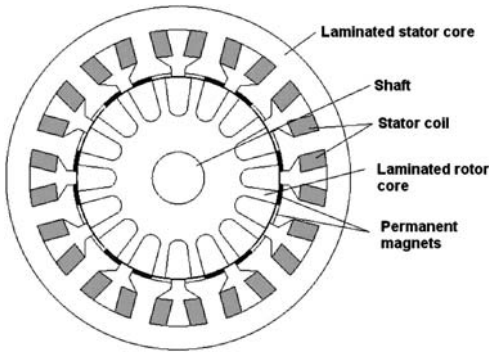

Figure 6. Cross-section of 12/16 pole CSPFRM.

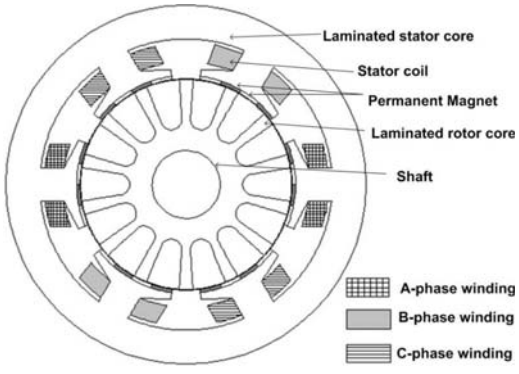

Figure 7. Cross-section of 6/14 pole CSPFRM.

Phase flux linkage variation of CSPFRM and FPFRM with the same physical dimensions and number of turns is shown in figure 9. The figure clearly shows that stator flux linkage in FPFRM is twice as that in CSPFRM. This results in high power density (More & Fernandes 2007). Two machines are designed for the proof of this concept, one with full pitch winding arrangement and the other with concentrated stator pole winding. Both machines have identical power and speed rating.

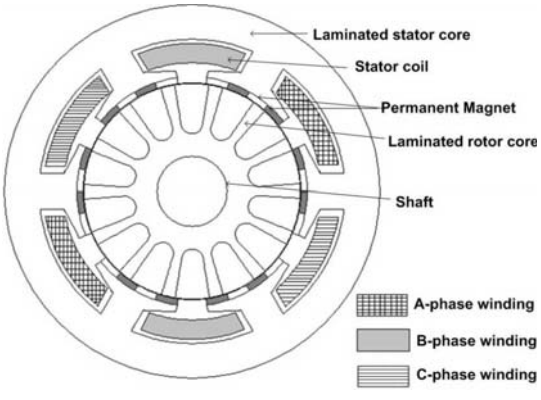

Figure 8. Cross-section of 6/14 pole FPFRM.

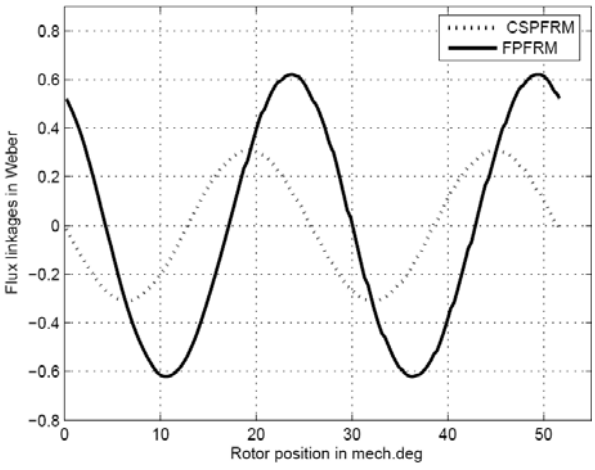

Figure 9. Phase flux Linkages in 6/14 pole CSPFRM and FPFRM.

4. Design details of CSPFRM and FPFRM for low speed application

FRM machine configurations suitable for 300 rpm are:

- 12/16 pole configuration.
- 6/14 pole configuration.

The above configurations are shown in figures 6 and 7 respectively and their comparison is shown in table 1. It is observed that 6/14 pole configuration has effective flux pattern of 2 poles, where as 12/16 configuration has flux pattern of 4 poles as shown in figures 10 and 11 respectively. Stator flux linkage in 6/14 pole configuration is twice as that of 12/16 pole configuration for same magnet volume, physical dimensions and number of turns. Therefore 6/14 pole configuration has higher power density than 12/16 pole configuration. Hence, 6/14 pole FRM configuration is selected. Detailed specifications of FRM is given in table 2.

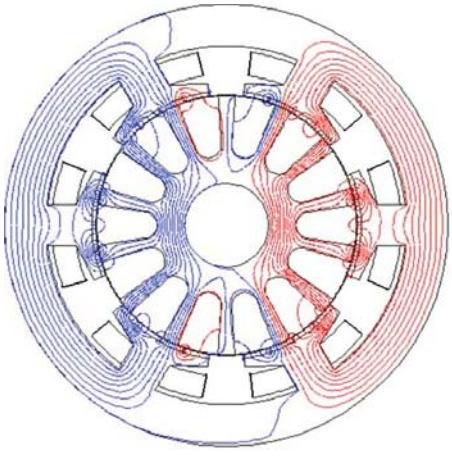

Figure 10. Flux pattern in 6/14 pole CSPFRM.

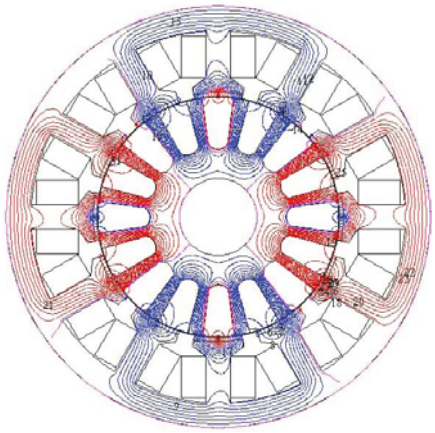

Figure 11. Flux pattern in 12/16 pole CSPFRM.

Table 1. Flux pattern poles for various FRM configurations.

Sr. No.	Machine type	No. of magnets	Gear ratio	No. of Flux pattern poles
1	6/8 pole	12	8	2
2	**12/16 pole**	**24**	**8**	**4**
3	**6/14 pole**	**24**	**14**	**2**
4	12/28 pole	48	14	4
5	12/40 pole	60	20	4

4.1 *Sizing of FRM*

A procedure for sizing of FRM is given in Boldea *et al* (2002). Specific electrical and magnetic loading will determine the specific tangential force f_t. Relationship between machine dimensions and torque is given by

$$T_e = f_t \pi D_r l_{sk} \frac{D_r}{2}, \tag{4}$$

Table 2. Specifications of 6/14 pole FRM.

Sr. No.	Description	Symbol	Value
1	Torque of the machine (Nm)	T_e	89
2	Rated phase voltage (V)	V_{ph}	96
3	Rated speed (rpm)	N	300
4	Rated current (A)	I	10
5	Frequency (Hz)	f	70
6	Number of stator poles	P_s	6
7	Number of rotor poles	P_r	14
8	Number of magnet pairs per stator pole	n_{pp}	2

where, D_r = diameter of the rotor.
l_{sk} = stack length of the machine.
The ratio of stack length to rotor diameter λ is defined as

$$\lambda = \frac{l_{sk}}{D_r}. \tag{5}$$

From equations 4 and 5 the rotor diameter is given by

$$D_r = \sqrt[3]{\frac{2T_e}{\pi f_t \lambda}}. \tag{6}$$

The PM flux per stator pole ϕ_{PM} is given by

$$\phi_{PM} = l_{sk} \cdot B_{PMi} \cdot \tau_{PM} \cdot n_{pp} \cdot K_{fringe}, \tag{7}$$

where, n_{pp} = number of magnet pairs per stator pole.
K_{fringe} = ratio of flux linking the stator winding to airgap flux.
τ_{PM} = permanent magnet pole arc length.
The ideal flux density in the airgap B_{PMi} is given by

$$B_{PMi} = B_r \frac{h_{PM}}{h_{PM} + g}, \tag{8}$$

where, B_r = remainent flux density of PM
h_{PM} = permanent magnet thickness.
g = airgap thickness.
FEM analysis shows that the variation of stator flux linkage is almost sinusoidal with rotor position θ_r.

$$\phi_{PM}(\theta_r) = \phi_{PM} \sin(P_r \theta_r) \tag{9}$$

$$\frac{d\phi_{PM}(\theta_r)}{d\theta_r} = l_{sk} \cdot B_{PMi} \cdot \tau_{PM} \cdot n_{pp} \cdot K_{fringe} \cdot P_r \cdot \cos(P_r \theta_r). \tag{10}$$

There are $\frac{P_s}{3}$ stator poles per phase and $\frac{P_s}{3}$ coils in series with n_c turns per coil. The EMF amplitude per phase is

$$E_m = \frac{P_s}{3} \cdot n_c \cdot 2 \cdot \pi \cdot n \cdot l_{sk} \cdot B_{PMi} \cdot \tau_{PM} \cdot n_{pp} \cdot K_{fringe} \cdot P_r. \tag{11}$$

The generalized equation applicable to three-phase flux reversal machines is given by

$$E_m = \frac{P_s}{3} \cdot n_c \cdot 2 \cdot \pi \cdot n l_{sk} \cdot B_{PMi} \cdot \tau_{PM} \cdot K_{fringe} \cdot n_{pp} \cdot P_r \cdot K_{wt}, \tag{12}$$

where, K_{wt} is winding type factor that depends upon the type of winding in FRM (i.e. concentrated stator pole winding and full pitch winding). Value of K_{wt} for both windings is shown in table 3.

In constant torque region, FRM is controlled by maintaining $I_d = 0$. The rated phase current of the machine is given by

$$I = \frac{2\pi n T_e}{\frac{3E_m}{\sqrt{2}}}. \tag{13}$$

Table 3. Value of K_{wt} for different types of FRM winding.

Sr. No.	Description	Value
1	Concentrated stator pole winding	1·0
2	Full pitch winding	2·0

Having determined the number of turns per coil and phase current, the slot area required for the winding is obtained by considering the slot fill factor (K_{fill}) and winding current density (j_{cn}). The slot area is given by

$$A_{slot} = \frac{2n_c I}{j_{cn} K_{fill}}. \tag{14}$$

Stator pole width is decided based on magnet width τ_{PM} and flux density in stator pole. Stator slot area determines the stator pole height. Stator core width is taken to be equal to stator pole width, and stator pole arc to pole pitch ratio is taken as 0·75 for 6/14 pole CSPFRM (Wang *et al* 1999). Two magnet pole pairs per stator pole are used. The rotor pole span is taken as 120° electrical and the airgap between stator and rotor is 0·5 mm. Magnet thickness is 2·5 mm.

4.2 *Dimensions of CSPFRM*

The main dimensions of 6/14 pole, 2·4 kW (88·58 Nm) CSPFRM are determined using the procedure given above. Following data is assumed for the design of the machine.

- Specific force $f_t = 1{\cdot}6\,\text{N/cm}^2$
- $\lambda \approx 1{\cdot}0$
- Efficiency of the machine = 86%
- PM remnant flux density $B_r = 1{\cdot}2$ Tesla
- Flux leakage factor $K_{fringe} = 0{\cdot}44$
- Slot fill factor $K_{fill} = 0{\cdot}3$
- Winding current density $j_{cn} = 3{\cdot}5\,\text{Amps/mm}^2$.

The dimensions of 6/14 pole, 88·58 Nm, 300 rpm CSPFRM is given in table 4. The overall dimensions of the machine are shown in the figure 12a.

4.3 *Dimensions of FPFRM*

Design equations for CSPFRM and FPFRM are same except the voltage per turn. Voltage induced in FPFRM is twice as that in CSPFRM for same magnetic and electrical loading. In order to reduce the material and manufacturing cost, physical dimensions (cross section and number of turns) of both machines are taken to be the same except the stack length. For the same physical dimensions and power, the stack length of FPFRM is ideally half of that of CSPFRM. However the FPFRM has higher voltage regulation due to higher value of inductance. In order to obtain same torque (power output), stack length of FPFRM is increased by 13% of its ideal length. This stack length is 56·6% of CSPFRM. Thus the stack length of FPFRM is 85 mm. The overall dimensions of the machine are shown in the figure 12b.

Table 4. Dimensions of 6/14 pole, 88·58 Nm, 300 rpm CSPFRM.

Sr. No.	Description	Symbol	Value
1	Airgap (mm)	g	0·5
2	Magnet thickness (mm)	h_{pm}	2·5
3	Rotor pole span angle (° mech.)	β_r	7·5°
4	Stator pole span angle (° mech.)	β_s	45°
5	Stator pole span (mm)	τ_{ps}	63·2
6	Rotor pole span (mm)	τ_{pr}	10·2
7	Stator pole height (mm)	h_{ps}	27
8	Rotor pole height (mm)	h_{pr}	30
9	Outer diameter of rotor (mm)	D_i	155
10	Outer diameter of stator (mm)	D_o	264
11	Number of turns/phase	N_{ph}	132
12	Stack length of machine (mm)	l_{sk}	150
13	Stator pole width (mm)	W_{sp}	25
14	Stator core width (mm)	W_{sc}	25
15	Shaft diameter (mm)	D_{sh}	50

4.4 *Iron Loss of CSPFRM and FPFRM*

FEM analysis is used to determine the flux density and frequency of the flux reversal in each part of the machine. Cold rolled non grain oriented silicon steel lamination (CRNGO) of 0·5 mm thick M-36 grade is used for constructing the machine. Specific iron loss for each part of the machine is decided based on flux density and frequency of flux reversal. Table 5 shows the iron loss in each part of CSPFRM calculated from specific iron loss and weight of laminations. The calculated total iron loss is 59 W and total weight of laminations is 39 Kg.

Stack length of CSPFRM and FPFRM is 150 mm and 85 mm respectively. The core loss in FPFRM is 33·50 W and weight of the core is 22·15 Kg.

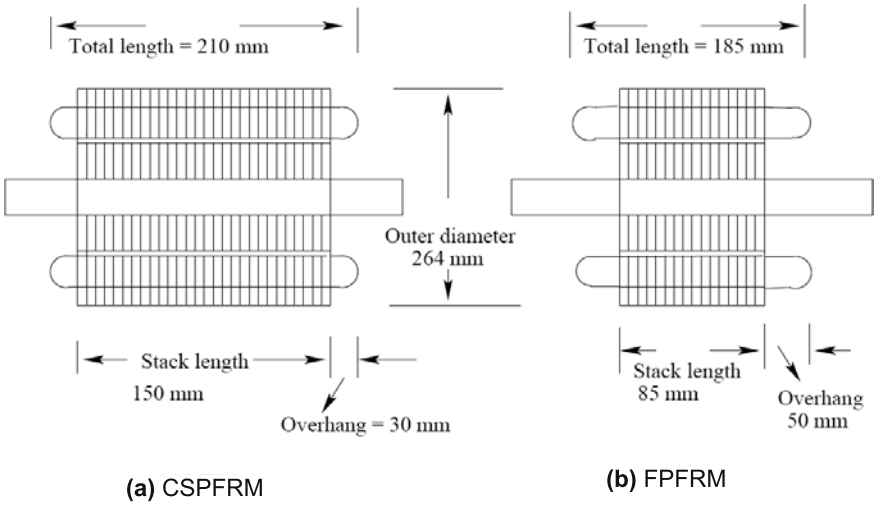

Figure 12. Overall dimensions of CSPFRM and FPFRM.

Table 5. Iron loss of 6/14 pole CSPFRM.

Sr. No.	Machine part	flux density Wb/m^2	Frequency Hz	Specific loss W/Kg	Weight Kg.	Iron loss Watts
1	Rotor core	0·8	65	1·79	5·88	10·5
2	Rotor pole	0·8	65	1·79	4·93	8·82
3	Stator core	0·6	70	1·17	21·53	25·19
4	Stator pole	0·6	70	1·17	2·92	3·416
5	Stator pole shoe	1·0	70	2·98	3·75	11·175

4.5 *Winding Resistance and Copper Loss of FPFRM and CSPFRM*

Number of turns and cross-section of the conductor is same in both the machines. However stack length and end turn overhang are different. Overhang of FPFRM is higher, which results in higher resistance and copper loss. The details of winding resistance, copper loss and copper weight for both machines are given in table 6.

5. Self and mutual inductance of CSPFRM and FPFRM

Self and mutual inductances are calculated using FEM analysis. Variation of self inductance of 6/14 pole CSPFRM and FPFRM with rotor position is shown in figure 13. It is observed that the ratio of self inductance of FPFRM to CSPFRM is 1·6.

The variation of mutual inductance between the phases of FPFRM and CSPFRM is shown in figure 14. The mutual inductance between the phases of CSPFRM is very low (i.e. 0·44 mH to 0·56 mH). This inductance between the phases of FPFRM varies with rotor position. These values for both machines obtained from FEM are shown in table 7.

6. Voltage regulation of the machine

Voltage regulation of FPFRM and CSPFRM generator for resistive load are obtained at 300 rpm with FEM simulation. The no load voltages of CSPFRM and FPFRM are 96·76 volt and 109·8 volt respectively. Figure 15 shows the variation of terminal voltage with load of both machines. The regulation of both machines is poor due to armature reaction. Series capacitive compensation is provided for both machines to improve the voltage regulation. The

Table 6. Winding data of 6/14 pole CSPFRM and FPFRM.

Sr. No.	Parameter	CSPFRM	FPFRM
1	Winding resistance per phase (Ohm)	0·3928	0·6363
2	Copper loss (Watt)	120.00	195·50
3	Copper weight (Kg)	5·1498	8·29
4	Magnet weight (Kg)	1·10	0·623

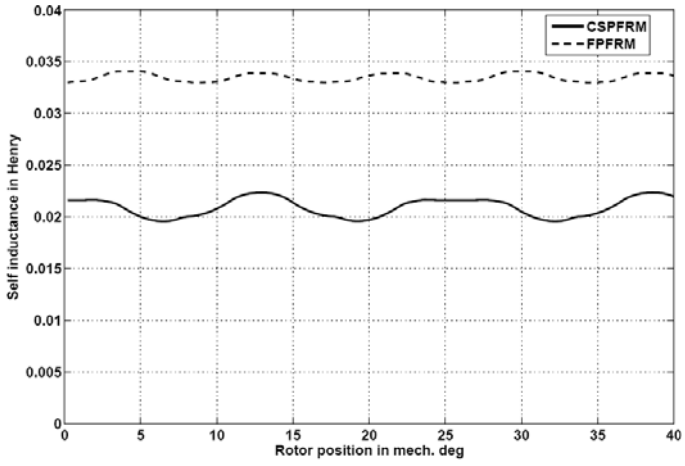

Figure 13. Variation of self inductance with rotor position for 6/14 pole CSPFRM and FPFRM.

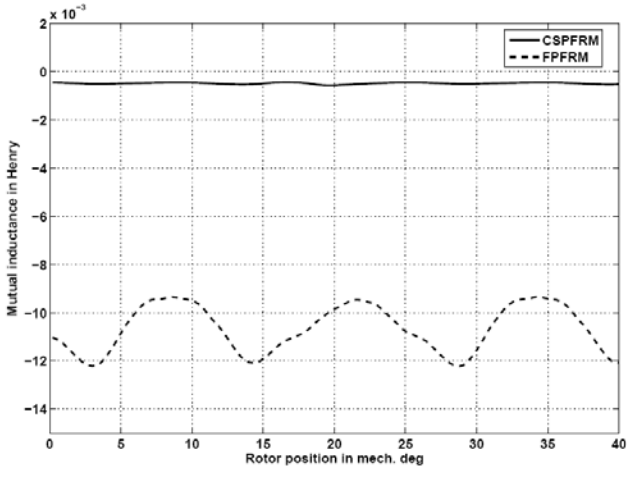

Figure 14. Variation of mutual inductance with rotor position for 6/14 pole CSPFRM and FPFRM.

Table 7. Self and mutual inductance of 6/14 pole CSPFRM and FPFRM.

Sr. No.	Parameter	CSPFRM	FPFRM
1	Self inductance with FEM analysis (min. value) in mH	19·57	32·96
2	Self inductance with FEM analysis (max. value) in mH	22·33	34·07
3	Mutual inductance with FEM analysis (min. value) in mH	0·44	9·35
4	Mutual inductance with FEM analysis (max. value) in mH	0·56	12·22

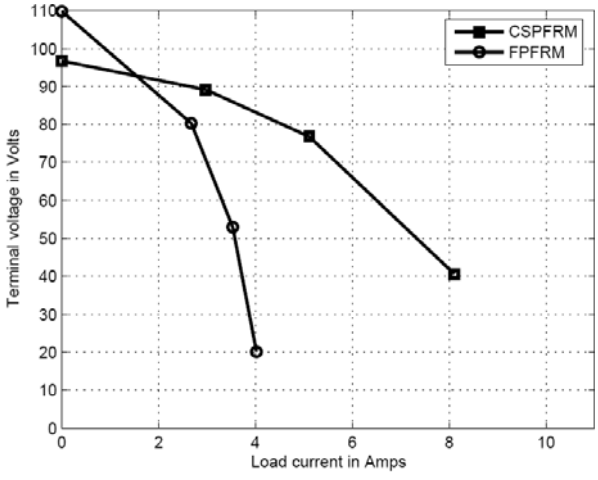

Figure 15. Voltage regulation characteristics of 6/14 pole CSPFRM and FPFRM.

uncompensated regulation characteristic is used to calculate the value of synchronous inductance L_s, which is used to determine the size of capacitor for series capacitive compensation of the machine.

Voltage regulation of FPFRM and CSPFRM is improved with series capacitive compensation. The value of series capacitance is given by Naoe (1997); Wang *et al* (2001).

$$C = \frac{1}{\omega^2 \times L_s}, \tag{15}$$

where $\omega =$ output frequency of voltage (rad/sec).
$L_s =$ synchronous inductance of the machine/phase (H) .
The regulation characteristics for compensated CSPFRM and FPFRM are shown in figure 16.

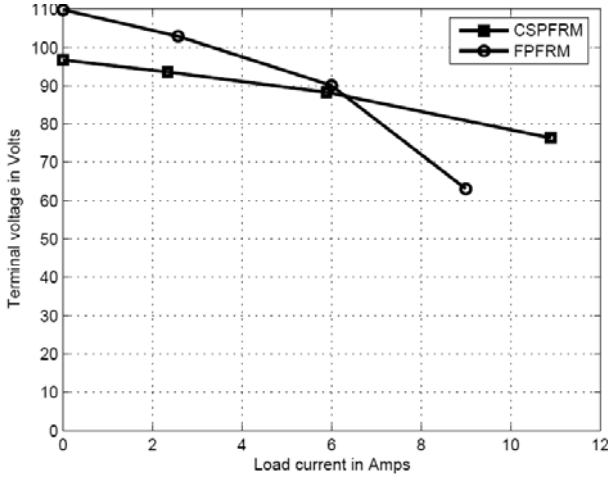

Figure 16. Variation of voltage regulation with load for 6/14 pole compensated CSPFRM and FPFRM.

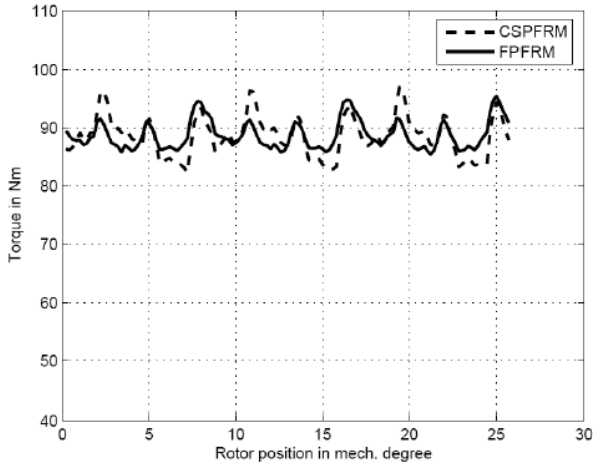

Figure 17. Steady state torque of 6/14 pole CSPFRM and FPFRM at rated current.

The values of compensating capacitors for CSPFRM and FPFRM are 195 μF and 85·66 μF respectively.

7. Steady state motor performance of FPFRM and CSPFRM

FEM simulation is carried out on both machines to determine the developed torque at rated current. At rated speed, the torque produced by the machine is obtained by aligning the stator current along q-axis (i.e. $I_d = 0$) (Gieras & Wing (2002), Miller (1989).

The variation of steady state torque produced by both machines with rotor position is shown in figure 17. The minimum and maximum values of torque for CSPFRM are 82 Nm and 97·2 Nm respectively. These values for FPFRM are 85·44 Nm and 95·44 Nm respectively. The average value of torque for CSPFRM is 88·57 Nm and FPFRM is 88·74 Nm.

Voltage required to drive the motor at rated current are different for both machines. The rms AC voltages required for CSPFRM and FPFRM are 138 volts and 226 volts respectively. The waveforms of voltages required to supply sinusoidal current into the machine is shown in

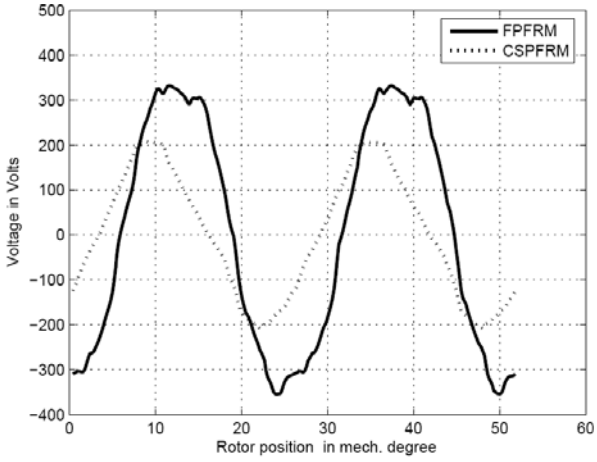

Figure 18. Phase voltage waveforms of 6/14 pole CSPFRM and FPFRM at rated current.

Table 8. Comparison of motor performance of 6/14 pole CSPFRM and FPFRM.

Sr. No.	Parameter	CSPFRM	FPFRM
1	Phase voltage (V)	138.00	226.00
2	Torque (Nm)	89.00	89.00
3	Active weight of the machine (Kg)	45·30	31.00
4	Torque to weight ratio (Nm/Kg)	1·96	2·87

figure 18. Comparison of both machines is given in table 8. From this table it can be inferred that torque to weight ratio of FPFRM is 1·46 times the CSPFRM. The cost of FPFRM is less as material cost is less. Thus FPFRM is low cost, high power density machine as compared to CSPFRM.

8. Conclusion

The design details of CSPFRM and FPFRM are presented. FEM analysis is carried out to evaluate the performance of these machines. Self inductance of FPFRM is approximately 1·6 times that of CSPFRM which resulted in poor voltage regulation. Series capacitive compensation is provided to improve the voltage regulation. Motor performance of both machines is evaluated with FEM and it showed that the torque produced by both machines are approximately equal. Torque to weight ratio of FPFRM is 1·46 times higher than CSPFRM and cost of FPFRM is less as material cost is less. Hence it could be concluded that FPFRM is a low cost, high power density machine as compared to CSPFRM.

References

Boldea Ion, Zhang Jichum, Nasar S A 2002 Theoretical characterization of flux reversal machine in low speed servo drives-The pole PM configuration. *IEEE Trans. Industry Applications* 38(6) 1549–1557

Deodhar R P, Anderson Savante, Boldea Ion, Miller T J E 1997 The flux reversal machine: A new doubly salient permanent magnet machine. *IEEE Trans. Industry Applications* 33(4): 925–934

Gieras J F, Wing M 2002 Permanent Magnet Motor Technology Design and Applications. Marcel Dekker Inc.

Kim Tae Heoung, Lee Ju 2004 A study of the design for the flux reversal machine. *IEEE Trans. on Magnetics.* 40(4): 2053–2055

Kim Tae Heoung, Sung Hong Won, Ki Bong, Ju Lee 2005 Reduction in cogging torque in flux reversal machine by rotor teeth pairing. *IEEE Trans. on Magnetics* 41(10): 3964–3966

Miller T J E 1989 Brushless permanent magnet and reluctance motor drives. (Oxford: Clarendon Press)

More D S, Fernandes B G 2007 Novel three phase flux reversal machine with full pitch winding. *Proc. of International Conference on Power Electronics (ICPE 2007)* Daegu, South Korea 1007–1012

Naoe Nobuyuki 1997 Voltage compensation of permanent Magnet generator with capacitors. *Proc. of IEEE Electrical Machines and Drives* wb2·14·1–wb2·14·3

Wang C, Nasar S A, Boldea I 1999 Three phase flux reversal machine (FRM). *IEE Trans. Electrical Power Application* 146(2) 139–146

Wang C, Boldea I, Nasar S A 2001 Characterization of three-phase flux reversal machine as an automotive generator. *IEEE Trans. on Energy Conversion* 16(1): 74–80

Zhang Jianzhong, Cheng Ming, Hua Wei, Zhu Xiaoyong 2006 New approach to power equation for comparison of doubly salient electrical machines. *Proc. IEEE Industry Applications Annual. Meeting* 1178–1185

CEDRAT France Flux 2D FEM Software (www.cedrat.com)